34th Annual International Conference of the IEEE EMBS
San Diego, California USA, 28 August - 1 September, 2012

Performance Bounds for Dynamic Causal Modeling of Brain Connectivity

Shun Chi Wu and A. Lee Swindlehurst

***Abstract*— The use of complex dynamical models have been proposed for describing the connections and causal interactions between different regions of the brain. The goal of these models is to accurately mimic the event-related potentials observed by EEG/MEG measurement systems, and are useful in understanding overall brain functionality. In this paper, we focus on a class of nonlinear dynamic causal models (DCM) that are described by a set of connectivity parameters. In practice, the DCM parameters are inferred using data obtained by an EEG or MEG sensor array in response to a certain event or stimulus, and the resulting estimates are used to analyze the strength and direction of the causal interactions between different brain regions. The usefulness of the parameter estimates will depend on how accurately they can be estimated, which in turn will depend on noise, the sampling rate, number of data samples collected, the accuracy of the source localization and reconstruction steps, *etc*. The goal of this paper is to derive Cramér-Rao performance bounds for DCM estimates, and examine the behavior of the bounds under different operating conditions.**

I. Introduction

Recent research in understanding brain functionality has focused on describing the connectivity between different cortical regions and how these regions interact when executing certain sensorimotor and cognitive tasks. One approach to this problem endeavors to find a specific parametric model that represents the simplest brain circuit that would produce the same event-related potentials (ERP's) measured experimentally by electroencephalography (EEG) or magnetoencephalography (MEG) systems. In order to do this, one must postulate a suitable causal model in which the regions of interest are constrained by a combination of neuroanatomical, neuropsychological and functional neuroimaging data [1], [2], [3]. Dynamic causal modeling (DCM) [4], [5], [6], [7] based on the neural mass model of [8] is an example of this approach. In DCM, the brain is regarded as a nonlinear dynamical network. Each cortical region in the DCM network is comprised of three subpopulations linked by intrinsic connections, and different regions communicate through extrinsic excitatory forward, backward and lateral connections. The activity of each cortical area is described by unobserved state variables and the output of the model is presumed to be the sources of the EEG/MEG ERPs.

The goal of this paper is to discuss dynamic causal modeling for brain connectivity from an estimation theoretic viewpoint. After presenting the DCM approach in the next section, we develop a method for obtaining the Cramér-Rao bound (CRB) [9] for the DCM parameters in Section III. In general, calculation of the CRB requires evaluation of the Fisher information matrix, which involves derivatives of the probability distribution function (pdf) of the measurements with respect to the parameters. However, the nonlinear differential equation at the heart of DCM does not admit an analytical description of the effect of the model parameters on the output, so standard methods cannot be used. Instead, we calculate the posterior CRB using the "derivative system" approach in [10]. The results of several numerical examples are given in Section IV to indicate DCM estimation performance as a function of signal-to-noise ratio (SNR) and sampling rate.

Shun Chi Wu is with the Department of Electrical Engineering and Computer Science, University of California, Irvine, CA 92697 USA scwu@uci.edu

A. Lee Swindlehurst is with the Department of Electrical Engineering and Computer Science, University of California, Irvine, CA 92697 USA swindle@uci.edu

II. Dynamic Causal Modeling for ERP Generation

Following the dynamic model of [8], [5], [6], the activity of the i^{th} cortical region is described by an eight-element state vector $\mathbf{x}^{(i)}(t) = [x_1^{(i)}(t) \dots x_8^{(i)}(t)]^T$ whose evolution is governed by the following nonlinear differential equation:

$$\begin{aligned} \dot{\mathbf{x}}^{(i)}(t) &= \mathbf{f}^{(i)}(t) \\ y_s^{(i)}(t) &= x_2^{(i)}(t) - x_3^{(i)}(t), \end{aligned} \tag{1}$$

where the elements of the vector $\mathbf{f}^{(i)}(t) = [f_1^{(i)}(t) \ \dots \ f_8^{(i)}(t)]^T$ are specified as

$$\begin{aligned} f_1^{(i)}(t) &= x_4^{(i)}(t), \\ f_2^{(i)}(t) &= x_5^{(i)}(t), \\ f_3^{(i)}(t) &= x_6^{(i)}(t), \\ f_4^{(i)}(t) &= \frac{H_e}{\tau_e}\{ \sum_{j=1;j\neq i}^{m} a_{ij}^F S(y_s^{(j)}(t-\delta_{ij})) \\ &+ \sum_{j=1;j\neq i}^{m} a_{ij}^L S(y_s^{(j)}(t-\delta_{ij})) + c_i u_i(t) \\ &+ \gamma_1 S(y_s^{(i)}(t))\} - \frac{2}{\tau_e} x_4^{(i)}(t) - \frac{x_1^{(i)}(t)}{\tau_e^2}, \end{aligned}$$

$$
\begin{aligned}
f_5^{(i)}(t) &= \frac{H_e}{\tau_e}\{\sum_{j=1;j\neq i}^{m} a_{ij}^B S(y_s^{(j)}(t-\delta_{ij})) \\
&+ \sum_{j=1;j\neq i}^{m} a_{ij}^L S(y_s^{(j)}(t-\delta_{ij})) \\
&+ \gamma_2 S(x_1^{(i)}(t))\} - \frac{2}{\tau_e}x_5^{(i)}(t) - \frac{x_2^{(i)}(t)}{\tau_e^2}, \\
f_6^{(i)}(t) &= \frac{H_i}{\tau_i}\gamma_4 S(x_7^{(i)}(t)) - \frac{2}{\tau_i}x_6^{(i)}(t) - \frac{x_3^{(i)}(t)}{\tau_i^2}, \\
f_7^{(i)}(t) &= x_8^{(i)}(t), \\
f_8^{(i)}(t) &= \frac{H_e}{\tau_e}\{\sum_{j=1;j\neq i}^{m} a_{ij}^B S(y_s^{(j)}(t-\delta_{ij})) \\
&+ \sum_{j=1;j\neq i}^{m} a_{ij}^L S(y_s^{(j)}(t-\delta_{ij})) \\
&+ \gamma_3 S(y_s^{(i)}(t))\} - \frac{2}{\tau_e}x_8^{(i)}(t) - \frac{x_7^{(i)}(t)}{\tau_e^2}.
\end{aligned}
$$

The parameters of the differential equation are explained below. The constant c_i represents the strength of the influence of the input excitation $u_i(t)$, which may not be present in all modeled brain regions. Parameters a_{ij}^F, a_{ij}^B, a_{ij}^L define the connectivity of the extrinsic forward, backward, and lateral connections between regions i and j, respectively, while δ_{ij} represents the conduction delay between the two regions. The coupling parameters $\gamma_1, \ldots, \gamma_4$ control the strength of the intrinsic connections between the three subpopulations within each brain region, and are proportional to the average number of synapses between the pyramidal cells and the excitatory and inhibitory feedback elements. The remaining constants are relevant to two transformations on which the system dynamics are based. The first transformation is linear and converts the average pulse density of the action potentials arriving at the population of neurons into an average postsynaptic membrane potential. In particular, H_e and H_i control the maximum postsynaptic potentials, and τ_e and τ_i represent the lumped time constants of the passive membrane and all other spatially distributed delays in the dendritic network. The subscripts e and i are used to indicate whether these potentials are either excitatory and inhibitory, respectively. The second transformation $S(v)$ is a nonlinear sigmoid function that converts the average membrane potential of the given population into an average firing rate for the action potentials, and is given by [5]

$$
S(v) = \frac{2e_0}{1+e^{(-rv)}} - e_0 \ , \tag{2}
$$

where e_0 determines the maximum firing rate of the neural population and r controls the steepness of the sigmoidal transformation.

For a general DCM network composed of m interconnected brain regions, a network-level model is obtained by combining together all of the equations for each region into a single nonlinear differential equation with $8m$ states:

$$
\begin{aligned}
\dot{\mathbf{x}}(t) &= \mathbf{f}(t) \\
\mathbf{y}(t) &= \mathbf{C}\mathbf{x}(t) + \mathbf{w}(t) = \mathbf{y}_s(t) + \mathbf{w}(t)
\end{aligned} \tag{3}
$$

where $\mathbf{x}(t) = [(\mathbf{x}^{(1)}(t))^T \ldots (\mathbf{x}^{(m)}(t))^T]^T$ and $\mathbf{f}(t) = [\mathbf{f}^{(1)}(t)^T \ldots \mathbf{f}^{(m)}(t)^T]^T$ represents the network state vector and its derivatives, $\mathbf{u}(t) \in \mathbb{R}^{m\times 1}$ contains the external inputs to each region (some of which may be zero), and $\mathbf{y}(t) \in \mathbb{R}^{m\times 1}$ represents the measured ERPs for each region in the presence of measurement noise $\mathbf{w}(t) \in \mathbb{R}^{m\times 1}$. In deriving the CRB, we will assume that $\mathbf{w}(t)$ is zero-mean Gaussian with independent elements of equal variance σ^2. The noise free ERPs are represented as $\mathbf{y}_s(t) = \mathbf{C}\mathbf{x}(t) = [y_s^{(1)}(t) \ldots y_s^{(m)}(t)]^T \in \mathbb{R}^{m\times 1}$, where $\mathbf{C} \in \mathbb{R}^{m\times 8m}$ is a constant matrix having with nonzero elements only in the following locations: $C_{i,8(i-1)+2} = 1$ and $C_{i,8(i-1)+3} = -1$ for $i = 1, \ldots, m$. Associated with the nonlinear state equations in (3) are a set of parameters represented by the vector $\boldsymbol{\theta}$. This vector contains the unknown extrinsic parameters $a_{ij}^F, a_{ij}^B, a_{ij}^L, \delta_{ij}, c_i$ for each cortical region i and every region j to which i is connected.

III. CRB for Estimation in Nonlinear Systems

Let $\mathbf{Y} = [\mathbf{y}(t_1) \ldots \mathbf{y}(t_N)] \in \mathbb{R}^{m\times N}$ represent a matrix containing the ERPs for each of the m regions over N time samples. Assume the parameter vector $\boldsymbol{\theta}$ has n elements and denote the joint pdf of the data and parameters as $p(\mathbf{Y}, \boldsymbol{\theta})$. According to the CRB, a lower bound for the variance of an unbiased estimator $\hat{\boldsymbol{\theta}} = \mathbf{q}(\mathbf{Y})$ is given by

$$
\mathbf{V} \equiv E\left\{[\mathbf{q}(\mathbf{Y}) - \boldsymbol{\theta}][\mathbf{q}(\mathbf{Y}) - \boldsymbol{\theta}]^T\right\} \geq \mathbf{J}^{-1}, \tag{4}
$$

where the Fisher information matrix (FIM) $\mathbf{J}$ is $n \times n$ with elements

$$
\mathbf{J}_{ij} = E\left\{-\frac{\partial^2 \ln p(\mathbf{Y};\boldsymbol{\theta})}{\partial\theta_i \partial\theta_j}\right\} \quad i,j = 1, \ldots, n \ . \tag{5}
$$

Calculation of the FIM involves derivatives of a function of the nonlinear system outputs with respect to the parameters. Since an analytical expression for the DCM system output in terms of the parameters does not exist, these derivatives cannot be evaluated directly. Instead, we resort to the approach of [10], which shows that the FIM for a data set generated by a nonlinear system with additive Gaussian measurement noise can be expressed in terms of the outputs of its *derivative system*, which is also described by a set of nonlinear differential equations.

The derivative system for the DCM model in (3) is given by

$$
\begin{aligned}
\dot{\mathcal{X}}(t) &= \mathcal{F}(t) \\
\mathcal{Y}_{\boldsymbol{\theta}}(t) &= \mathcal{C}\mathcal{X}(t),
\end{aligned} \tag{6}
$$

for $t \geq t_0$, where

$$\mathcal{X}(t) = \left[\mathbf{x}^T(t) \ \frac{\partial \mathbf{x}^T(t)}{\partial \theta_1} \cdots \ \frac{\partial \mathbf{x}^T(t)}{\partial \theta_n}\right]^T \in \mathbb{R}^{8m(n+1)\times 1},$$

$$\mathcal{F}(t) = \begin{bmatrix} \mathbf{f}(t) \\ \frac{\partial \mathbf{f}(t)}{\partial \theta_1} + \mathbf{M}_J(t)\frac{\partial \mathbf{x}(t)}{\partial \theta_1} \\ \vdots \\ \frac{\partial \mathbf{f}(t)}{\partial \theta_n} + \mathbf{M}_J(t)\frac{\partial \mathbf{x}(t)}{\partial \theta_n} \end{bmatrix} \in \mathbb{R}^{8m(n+1)\times 1},$$

$$\mathcal{Y}_{\boldsymbol{\theta}}(t) = \begin{bmatrix} \frac{\partial y^{(1)}(t)}{\partial \boldsymbol{\theta}} \\ \vdots \\ \frac{\partial y^{(m)}(t)}{\partial \boldsymbol{\theta}} \end{bmatrix} = \begin{bmatrix} \frac{\partial (x_2^{(1)}(t) - x_3^{(1)}(t))}{\partial \boldsymbol{\theta}} \\ \vdots \\ \frac{\partial (x_2^{(m)}(t) - x_3^{(m)}(t))}{\partial \boldsymbol{\theta}} \end{bmatrix} \in \mathbb{R}^{mn\times 1}.$$

The matrix $\mathcal{C}$ is defined implicitly from the expression for $\mathcal{Y}_{\boldsymbol{\theta}}(t)$ and $\mathbf{M}_J(t) \in \mathbb{R}^{8m\times 8m}$ is the Jacobian matrix of $\mathbf{f}(t)$ with respect to $\mathbf{x}$. Once the derivative system is defined and initialized, standard numerical integration methods can be used to generate samples of the output and the FIM can then be obtained through

$$\mathbf{J}_D = \frac{1}{\sigma^2}\sum_{j=1}^{N}\sum_{i=1}^{m} \mathbf{P}_i \mathcal{Y}_{\boldsymbol{\theta}}(t_j)\mathcal{Y}_{\boldsymbol{\theta}}^T(t_j)\mathbf{P}_i^T \in \mathbb{R}^{n\times n}, \quad (7)$$

where $\mathbf{P}_i \in \mathbb{R}^{n\times mn}$ is defined as

$$\mathbf{P}_i = \left[\mathbf{0}^{(1)} \ \cdots \mathbf{0}^{(i-1)} \ \mathbf{I}_n \ \mathbf{0}^{(i+1)} \ \cdots \mathbf{0}^{(m)}\right],$$

with $\mathbf{0}^{(i)}$ being the i^{th} $n \times n$ zero matrix and $\mathbf{I}_n$ is an $n \times n$ identity matrix.

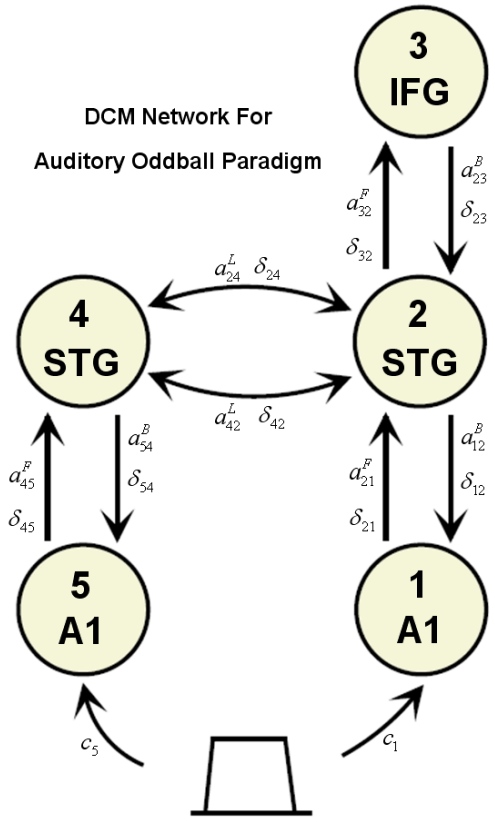

Fig. 1. A plausible DCM network for the auditory oddball paradigm.

IV. Simulations and Discussions

A. Simulation Setup and Parameters

To study the behavior of the DCM CRB, a DCM network [11] for investigating the underlying mechanism of the mismatch negativity (MMN) appearing in auditory oddball paradigm is adopted and depicted in Figure 1. Five lumped neural sources are assumed in this model ($m = 5$), two associated with the left and right primary auditory cortices (A1), two with the left and right superior temporal gyrus (STG) and one for the right inferior frontal gyrus (IFG). The model only includes the right-hemisphere IFG since it is reported to consistently produce stronger responses than the left IFG [11]. The audio cortices A1 (regions 1 and 5) receive the external audio stimulus from the ear canal via connections with unknown strength c_1, c_5. In the most general setting with all possible connections active, the audio cortices are linked to their respective ipsilateral STG (regions 2 and 4) with distinct forward and backward connection parameters $a_{21}^F, a_{12}^B, a_{45}^F, a_{54}^B$, and the conduction delays $\delta_{21}, \delta_{12}, \delta_{45}, \delta_{54}$ are assumed to be the same and equal to δ_1 for both pathways. The right STG is connected to the IFG with parameters a_{32}^F, a_{23}^B and conduction delay $\delta_{23} = \delta_{32} = \delta_2$. Inter-hemispheric or lateral connections between the left and right STG are defined by the parameters $a_{42}^L = a_{24}^L = a^L$ and $\delta_{24} = \delta_{42} = \delta_3$ (note that the forward and backward lateral connection strengths are assumed to be equal in the simulation since they exert much weaker effects on the system responses than forward and backward connections).

The parameter vector $\boldsymbol{\theta}$ of this DCM network is

$$\boldsymbol{\theta} = \left[a_{21}^F \ a_{32}^F \ a_{45}^F \ a_{12}^B \ a_{23}^B \ a_{54}^B \ c_1 \ c_5 \ a^L \ \delta_1 \ \delta_2 \ \delta_3\right]^T,$$

and Table I shows the value of the elements of $\boldsymbol{\theta}$ used in our simulation, which were tuned so that the the model generated ERP waveforms similar to those shown in [11]. Other DCM parameters were chosen to be similar to those used in prior work [8], [5], [6]: $H_e = 3.5\ mV$, $H_i = 32\ mV$, $\tau_e = 10\ ms$, $\tau_i = 15\ ms$, $\gamma_1 = 50$, $\gamma_2 = 40$, $\gamma_3 = \gamma_4 = 12.5$, $e_0 = 2.5\ s^{-1}$, $r = 0.56\ mV^{-1}$. The input signal to the audio cortices was a pulsed signal with a 70 ms duration and 5 ms rise and fall times, as depicted in Figure 1. The SNR in the results that follow is defined as $\|\mathbf{Y}_s\|_F^2/\|\mathbf{W}\|_F^2$, where $\mathbf{Y}_s = [\mathbf{y}_s(1), \ldots, \mathbf{y}_s(N)]$ and $\mathbf{W} = [\mathbf{w}(1), \ldots, \mathbf{w}(N)]$ represent the samples of the noise-free ERPs and the noise, respectively. In the results that follow, the SNR was varied from 5 to 20 dB. The DCM dynamic system and its derivative system were integrated using a fourth-order Runge-Kutta technique with an integration time-step specified by the sampling rate used with data collected during a 0.25 second time window.

B. Results and Discussions

Simulations in the first example were conducted with SNR varying from 5 to 20 dB and the sampling rate set at 1 kHz. The normalized CRB for each parameter, which is defined as the square root of the corresponding entry in the inverse

TABLE I

VALUES OF DCM NETWORK PARAMETERS USED IN SIMULATING THE AUDITORY ODDBALL PARADIGM.

Para.	a_{21}^F	a_{32}^F	a_{45}^F	a_{12}^B	a_{23}^B	a_{54}^B
value	40.56	61.42	31.75	8.67	13.81	8.81
Para.	c_1	c_5	a^L	δ_1	δ_2	δ_3
value	21.32	59.92	5.11	7.66	11.53	12.64

of the FIM divided by the value of the parameter itself, is provided in Figure 2. As expected, a decrease in SNR leads to an increase in the CRB and thus the root mean-squared error (RMSE) of any unbiased estimator. Among the elements of $\boldsymbol{\theta}$, δ_3 seems to be difficult to estimate accurately; for example, at an SNR of 5dB, the RMSE is larger than the value of δ_3 itself. In the second example, simulations were conducted with sampling rates varying from 200 to 1000 Hz and 10 dB SNR and the resulting CRB is plotted in Figure 3. We see that a reduction in sampling rate by a factor of five leads to an increase in the CRB of about a factor of two. It is clear from these examples how the CRB could be helpful in determining when meaningful inference could be made about the brain's behavior from the DCM estimates.

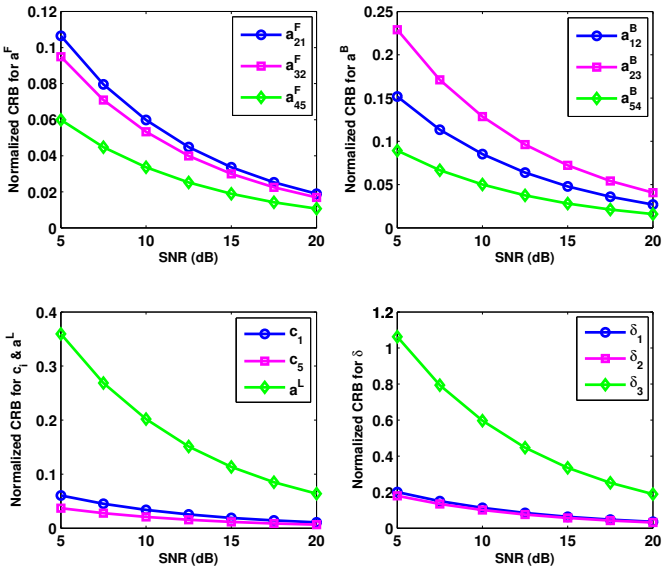

Fig. 2. Normalized CRB with 1 kHz sampling rate.

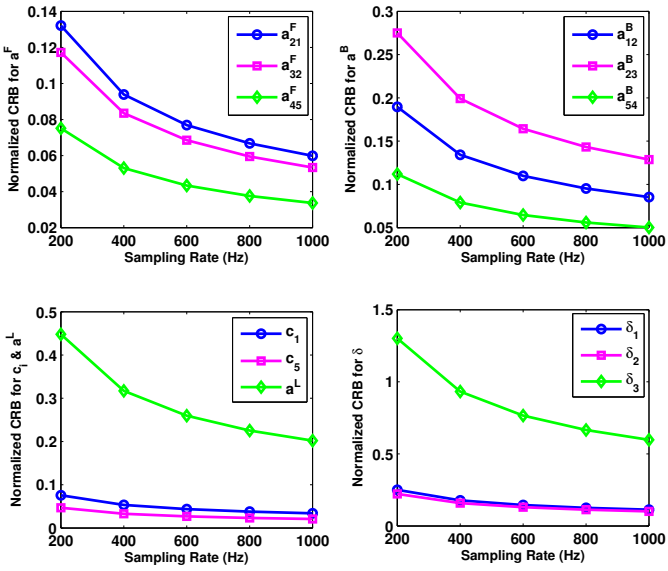

Fig. 3. Normalized CRB with 10 dB SNR.

V. CONCLUSIONS

We have presented a nonlinear DCM framework for generation of EEG/MEG ERPs and applied this framework for investigating the mechanism of the MMN observed in the auditory oddball paradigm. Under the DCM framework, the MMN can be inferred as being due to changes in forward and backward connections within the primary auditory cortex compared to those present under standard stimuli. However, to make such an inference, the ability to estimate the DCM parameters is required, which results in a nonlinear system identification problem. To address the question of how accurately the DCM parameters can be estimated, we derived the CRB for the DCM estimation problem, which required the definition of the derivative system associated with the DCM since it is impossible to explicitly express the log-likelihood in terms of the model parameters. The behavior of the CRB was studied as a function of SNR and sampling rate for the particular case of a DCM proposed for oddball auditory stimuli.

REFERENCES

[1] K. J. Friston, "Functional and effective connectivity in neuroimaging: a synthesis," *Human Brain Mapping*, vol. 2, pp. 56–78, 1994.

[2] L. Lee, L. M. Harrison, and A. Mechelli, "The functional brain connectivity workshop: report and commentary," *Neuroimage*, vol. 19, pp. 457–465, 2003.

[3] B. Horwitz, "The elusive concept of brain connectivity," *Neuroimage*, vol. 19, pp. 466–470, 2003.

[4] O. David and K. J. Friston, "A neural mass model for EEG/MEG: coupling and neuronal dynamics," *NeuroImage*, vol. 20, pp. 1743–1755, 2003.

[5] O. David, L. M. Harrison, and K. J. Friston, "Modelling event-related responses in the brain," *NeuroImage*, vol. 25, pp. 756–770, 2005.

[6] O. David, S. J. Kiebel, L. M. Harrison, J. Mattout, J. M. Kilner, and K. J. Friston, "Dynamic causal modeling of evoked responses in EEG and MEG," *NeuroImage*, vol. 30, pp. 1255–1272, 2006.

[7] K. E. Stephan and K. J. Friston, "Models of effective connectivity in neural systems," in *Handbook of Brain Connectivity*, V. K. Jirsa and A. R. McIntosh, Eds. Springer, 2007, pp. 303–327.

[8] B. H. Jansen and V. G. Rit, "Electroencephalogram and visual evoked potential generation in a mathematical model of coupled cortical columns," *Biol. Cybern.*, vol. 73, pp. 357–366, 1995.

[9] S. M. Kay, *Fundamentals of Statistical Signal Processing: Estimation Theory*. Prentice Hall, 1993.

[10] Z. Lin, Q. Zou, E. S. Ward, and R. J. Ober, "Cramervrao lower bound for parameter estimation in nonlinear systems," *IEEE Signal Processing Letter*, vol. 12, pp. 855–858, 2005.

[11] M. I. Garrido, J. M. Kilner, S. J. Kiebel, K. E. Stephan, and K. J. Friston, "Dynamic causal modelling of evoked potentials: A reproducibility study," *NeuroImage*, vol. 36, pp. 571–580, 2007.